Polymer Chemistry

Accepted Manuscript

ROYAL SOCIETY OF CHEMISTRY

www.rsc.org/polymers

Journal Name RSCPublishing

ARTICLE

Cite this: DOI: 10.1039/x0xx00000x

Novel multiarm star block copolymer ionomers as proton conductive membranes

Tuba ERDOGAN,*[a] Cigdem BILIR,[a,b] Elif UNVEREN,[a] A.Levent DEMIREL,[c] Umit TUNCA[b]

Received 00th January 2012,
Accepted 00th January 2012

DOI: 10.1039/x0xx00000x

www.rsc.org/

A series of well-defined novel multiarm star block copolymer ionomers with an average of 6, 11 and 15 arms, sulfonated polystyrene-*block*-poly(2,2,3,3,3-pentafluoropropyl methacrylate) (SPS-*b*-PFPMA), were prepared via a combination of atom transfer radical polymerization (ATRP), Diels–Alder click reaction and postsulfonation reaction. First, multiarm star polymer with anthracene functionality as reactive periphery groups was prepared by a cross-linking reaction of divinyl benzene using α-anthracene end functionalized PS (PS-anthracene) as a macroinitiator. Thus, obtained multiarm star polymer was then reacted with furan protected maleimide-end functionalized PFPMA (PFPMA-MI) resulting in the corresponding fluorinated multiarm star block copolymers via Diels–Alder click reaction. The third step concerned sulfonation reaction of phenyl ring of polystyrene block with acetyl sulfate at 20 °C. The structures, molecular characterization and thermal properties of the multiarm star block copolymers were characterized by using ^{1}H nuclear magnetic resonance (^{1}H NMR) and infrared (IR) spectroscopy, size exclusion chromatography (SEC), differential scanning calorimetry (DSC) and thermogravimetric analysis (TGA). Thermal analysis indicated separate glass transitions of the PFPMA and PS phases. Both the membranes from sulfonated multiarm star block copolymer and its sulfonated poly(phenylene oxide) (SPPO) blends were prepared by solution casting method. All of the multiarm star block ionomers were readily soluble in *N*,*N*-dimethyl acetamide. The influence of star functionality and ion exchange capacity (IEC) of star ionomers on the flexibility and the proton conductivity of ionomer membranes were examined. 6-arm star block copolymer ionomer membrane with 1.00 mmol/g IEC exhibited conductivity (19.37 mS/cm) higher than that of SPPO with 1.34 mmol/g IEC (3.82 mS/cm) measured at 80 °C and relative humidity of 100 %. The morphology of dry membranes was investigated by scanning electron microscopy (SEM). This work showed that it is possible to tailor and prepare proton exchange membrane with well-defined architecture by employing star block copolymers with a sulfonated core bearing hydrophobic fluorinated periphery.

Introduction

Fuel cell has been developed as a promising alternative for hydrogen energy conversion with high efficiency. Among various kinds of fuel cells, proton exchange membrane (also known as polymer electrolyte membrane) fuel cell (PEMFC) is considered as the most promising fuel cell techniques for automotive and portable power applications due to its simplicity in design and operational properties (1). Polymer electrolyte membrane (PEM) is the key element of PEMFC. The desired membrane properties should include high proton conductivity, good chemical and thermal stability, good mechanical strength, low fuel crossover and appropriate fabrication cost (2). None of the available membranes meets all of these requirements. Therefore, the synthesis of new membrane materials with improved properties is one of the ongoing research interests in polymer science (3). Nafion^{TM}, a perfluorosulfonate ionomer, is the most widely used PEM due to its outstanding properties; however; high cost, synthetic difficulty and environmental concerns about recycling have led to the investigation of novel membranes (4). Many polymeric structures as alternative membrane materials have appeared in the literature in the last several decades (3; 5-8). Block copolymer ionomers comprised of an ionic and nonionic block are the attractive candidates in PEM research due to their unique morphologies in the solid state that enhance the proton transport in the membrane (9). Well-defined sulfonated block copolymers can serve as model polymer systems to elucidation of relationships between morphology, microstructure and ionic conductivity in proton exchange membrane. Transport properties of the nanostructured membranes produced from polystyrene sulfonic acid containing block and graft copolymers have been extensively studied (9-12). Some key examples of sulfonated block copolymers include poly(styrene-*b*-[ethylene-*co*-butylene]-*b*-styrene) (S-SEBS) (13, 14), poly(styrene-*b*-isobutylene-*b*-styrene) (S-SIBS) (15-18), polystyrene-*b*-poly(ethylene-alt-propylene) (PS-PEP) (19), poly(styrene-*b*-methyl butene) (PSS-*b*-PMB) (20-22), poly(styrene-*b*-methyl methacrylate) (PSS-*b*-PMMA) (23,24), poly([norbornenyleneethylstyrene-*r*-styrene]-*b*-styrenesulfonic) (PNS-*b*-PSSA) (25), poly(hexyl methacrylate)-*b*-poly(styrene)-*b*-poly(hexyl methacrylate) (PHMA-*b*-PS-*b*-PHMA) (26). These sulfonated block copolymers generally have highly ordered sequence of both hydrophilic and hydrophobic blocks which gives the membrane enhanced proton conducting properties in relation to partially sulfonated random copolymer membranes. In graft copolymer studies, macromonomeric poly(styrene sulfonic acid) grafted polystyrene (PS-*g*-macPPSA) show enhanced conductivity compared to that of random copolymers of styrene and styrenesulfonic acid (PS-*r*-PSSA) (27-29). Other well-designed block copolymer ionomer structure including fluorinated hydrophobic block and polystyrene sulfonic acid as hydrophilic block have also increasingly been developed. Holdcroft and co-workers (30-35) have synthesized and investigated transport properties of several different block and graft copolymers, partially sulfonated poly([vinylidene difluoride-*co*-hexafluoropropylene]-*b*-styrene) (P-[VDF-*co*-HFP]-*b*-SPS), poly-([vinylidene difuoride-*co*-chlorotrifluoroethylene]-*g*-styrene)(P[VDF-*co*-CTFE]-*g*-SPS). These model fluorinated ionomers revealed the importance of polymer microstructure on the morphology of membranes; graft copolymer ionomer membranes possessed highly concentrated, and isotropically connected ionic domains in relation to diblock copolymer ionomer membrane which result more resistance to the excessive swelling and thus high proton conductivity. Among different architectures, proton conducting star block copolymers are the least investigated. Star-shaped SPS-*b*-polybutadiene copolymer ionomers were reported to show lower performance compared to Nafion® (36). Ueda and coworkers have synthesized star-shaped sulfonated block copolyetherketones having hydrophilic segments attached to the core, and the hydrophobic segments placed at the periphery of the star polymer (37). The star ionomer membranes showed high water uptake due to the star shaped structure and excellent proton conductivity which was comparable to that of Nafion 117 in the range of 50-95 % relative humidity at 80 °C. Although unique macromolecular structures such as graft, comb-shaped, and branched polymers were proposed as PEM materials for the elucidation of structure-property relationships (6), there is still a great demand for well-defined macromolecular structures being processed for this purpose.

In this spirit, we now turn our attention to study multiarm star block copolymer ionomers that are likewise capable of forming an inherent high water uptake molecular network due to the high density of sulfonic acid segments surrounded by hyrophobic segments. Herein, we report, for the first time, the synthesis of a series of novel multiarm star block ionomers containing hydrophobic fluorinated block at the periphery and partially sulfonated PS block at the core with varying ion exchange capacities (IECs). The star ionomer was designed to have incompatible two segments which are all tailored to afford self-assembly and ionic aggregation. Star block copolymers of partially sulfonated polystyrene-*block*-poly(2,2,3,3,3-pentafluoropropyl methacrylate) (SPS-*b*-PFPMA) with an average of 6, 11 and 15 arms were prepared via a combination of atom transfer radical polymerization (ATRP), Diels–Alder click reaction, followed by postsulfonation. Solvent cast membranes were characterized to further investigate the effect of the arm number and sulfonic acid content on properties including the water uptake, proton conductivity, and thermal and oxidative stability.

Experimental

Materials

Styrene (St, 99% Aldrich) and 2,2,3,3,3-pentafluoropropyl methacrylate (FPMA, 97%, Alfa Aesar) were passed through a basic alumina column to remove the inhibitor immediately prior to use. Divinylbenzene (DVB, 80%, Aldrich) was purified twice by passing through a column filled with basic alumina to remove the inhibitor. *N,N,N',N'',N''*-Pentamethyldiethylenetriamine (PMDETA, Aldrich) was distilled over NaOH prior to use. CuBr (99.9%, Aldrich), CuCl (99.9%, Aldrich) were used as received. Dichloromethane (CH_2Cl_2) was purchased from Aldrich and used after distillation over P_2O_5. Tetrahydrofuran (THF; 99.8%, J.T. Baker) was dried and distilled over benzophenone-Na. Other solvents were purified by conventional procedures. All other reagents were purchased from Aldrich and used as received.

Syntheses and Polymerizations

9-Anthyryl methyl 2-bromo-2-methyl propanoate, (38) **1**, 2-Bromo-2-methyl propionic acid 2-(3,5-dioxo-10-oxa-4-azatricyclo[5.2.1.02,6]dec-8-en-4-yl)-ethyl ester (39), **2** and anthracene-end functional PS (PS-anthracene) were synthesized according to published procedures and illustrated in Scheme 1.

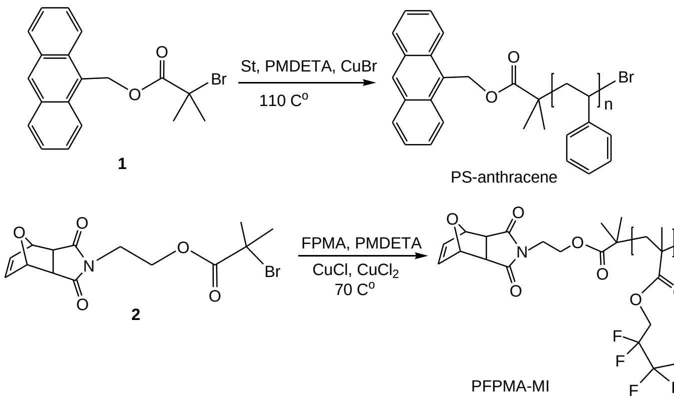

Scheme 1. Preparations of PS-anthracene by ATRP of St using **1** as an initiator and CuBr/PMDETA as a catalyst at 110 °C (^1H NMR ($CDCl_3$, δ) 8.44 (bs, 1H,

ArH of anthracene), 8.36 (bs, 2H, ArH of anthracene), 7.91 (bs, 2H, ArH of anthracene), 7.55 (bs, 4H, ArH of anthracene), 7.53–6.52 (ArH of PS), 5.87 (CH_2-anthracene), 4.44 (CH(Ph)-Br), 0.61–2.24 (aliphatic protons of PS); and furan protected maleimide-end functionalized PFPMA (PFPMA-MI) via ATRP of FPMA in the presence of **2** as an initiator, CuCl/PMDETA as a catalyst system at 70 °C.

Synthesis of α-furan protected maleimide end functionalized poly(2,2,3,3,3-pentafluoropropyl methacrylate) (PFPMA-MI)

PFPMA-MI was prepared by ATRP of PFMA. PFMA (6.0 mL, 35 mmol), PMDETA (0.073 mL, 0.35 mmol), CuCl (0.035 mL, 0.35 mmol), $CuCl_2$ (0.009 g, 0.07 mmol), toluene (6 mL), and 2(0.126 g, 0.35 mmol) were added in a Schlenk-tube and the reaction mixture was degassed by three vacuum/nitrogen cycles and left in nitrogen. The tube was then placed in a thermostated oil bath at 70 °C for 4 h. The polymer was dried for 24 h in vacuum oven at 30 °C. (Yield:4.72 g, $M_{n,SEC}$=10350 g/mol, $Đ$=1.21)

Synthesis of anthracene-end functionalized polystyrene-*block*-poly(divinyl benzene) star copolymer(($(PS)_m$-polyDVB))

PS-anthracene macroinitiator (10.5 g, 1.640 mmol), anisole (64.48 mL), PMDETA (342 μL, 1.640 mmol), DVB (3.504 mL, 24.60 mmol), and CuBr (235 mg, 1.640 mmol) were charged to a Schlenk tube equipped with a magnetic stirrer bar under argon atmosphere. The first sample was quickly taken from the reaction mixture for GC measurement, before it was degassed by using three freeze-pump-thaw (FPT) cycles. The reaction flask was back-filled with argon and immersed in a 110 °C oil bath. At timed intervals, samples were taken from the reaction mixture with argon purged-syringe under positive argon atmosphere. The samples were diluted with THF and purified by passing through short neutral alumina column to remove the copper salt and then filtered through poly(tetrafluoro ethylene) (PTFE) filter (0.2 μm pore size) prior to GC and GPC analyses. The reaction was stopped via exposure to air. The reaction mixture was diluted with THF, then filtered through a column filled with neutral alumina to remove the copper complex and the star polymer was precipitated in methanol. The crude product was dissolved in THF and then reprecipitated in methanol/diethyl ether mixture (1/1 v/v). Finally, the polymer was dried under vacuum at 30 °C for 24 h. (Yield:7.10 g).

"Diels–Alder" click reaction of anthracene-end functionalized polystyrene-*block*-poly(divinyl benzene) with PFPMA-MI: Preparation of PS-*b*-PFPMA multiarm star slock copolymers

A solution of PFPMA-MI (2.538 g, 0.02 mmol) in 60 mL of 1,4-dioxane was added to a 60 mL solution of multiarm anthracene-end functionalized $(PS)_m$-polyDVB (1.7 g 0.011 mmol) star polymer in toluene in a Schlenk tube. The mixture was bubbled with nitrogen for 45 min and refluxed for 62 h at 110 °C, and then toluene/1,4-dioxane was evaporated under vacuum. The crude product was dissolved in THF and precipitated into methanol. This procedure was repeated two times. The obtained white product was dried in a vacuum oven at 30 °C for 24 h. (Yield: 4.05g, $M_{n,SEC}$=85400 g/mol, $Đ$=1.39)

Sulfonation of Polymers

Sulfonation of multiarm star and star block copolymers was carried out in 1,2-dichloroethane (DCE) using the procedure described by Makowski et al. (40,41) except a reaction temperature of 20 C° was used. A typical sulfonation reaction is as follows: to a two-neck round-bottomed flask, 10 g. of star polymer was dissolved in 100 mL of DCE at 20 °C and purged with nitrogen for 45 min. Acetyl sulfate was prepared by the reaction of acetic anhydride and concentrated sulfuric acid at 0 °C in DCE. Then the freshly prepared acetyl sulfate was added dropwise to the polymer solution. The reaction flask was purged with nitrogen during the reaction. Commercially available poly(2,6-dimethyl-1,4-phenylene oxide) (PPO) was sulfonated using the same procedure described above except a reaction temperature of 30 °C and solvent of chloroform ($CHCl_3$) for the preparation of polymer solution were used. After the desired reaction time, 10 mL of methanol was slowly added to stop the reaction. The solution was evaporated under reduced pressure and the reaction product was recovered by precipitation in ice-cold deionized water. Sulfonated polymers were filtered, washed with deionized water until the pH of the washing water was neutral.

Membrane preparation

A 10-20 wt. % solution of multiarm star/star block ionomer in *N*,*N*-dimethylacetamide (DMAc) was prepared and filtered. For blend membrane preparation, multiarm star ionomer and SPPO were dissolved individually in DMAc and their blends with various compositions were prepared by mixing the polymer solutions. The solution was poured into a glass plate and stored at room temperature for 12 h. The residual solvent was evaporated in vacuum oven. The dried membrane was removed from the glass plate by immersing in deionized water and kept in water before being tested. The membrane thickness was measured at dry state using a digital micrometer. The thicknesses of fabricated membranes are in the range of 80-100 μm.

Instrumentation

^{1}H-NMR spectra were recorded on a Bruker NMR Spectrometer (400 MHz) in $CDCl_3$ (for unsulfonated polymers) and DMSO-d_6 (for sulfonated polymers) at room temperature. The conventional gel permeation chromatography measurements of unsulfonated polymers were obtained from an Agilent instrument (Model 1100) consisting of a pump, a refractive index (RI), and ultraviolet (UV) detectors, and three Zorbax columns (PSM60-S, PSM-300-S, PSM 1000-S). THF was used as an eluent at a flow rate of 0.4 mL/min at 30 °C. Toluene was used as an internal standard. The molecular weight of the polymers was calculated based on linear polystyrene standards (Polymer Laboratories). The three detection GPC (TD-GPC) set-up with an Agilent 1200 model isocratic pump, four Waters Styragel columns (guard, HR 5E, HR 4, HR 3, and HR 2), and a Viscotek TDA 302 triple detector including RI, dual laser light scattering (λ= 670 nm, 90° and 7°) and a differential pressure viscometer was conducted to measure the absolute molecular weights ($M_{w,TDGPC}$) in THF with a flow rate of 0.5 mL/min at 35 °C. Three detectors were calibrated with a PS Standard having narrow molecular weight distribution (M_n = 115,000, M_w/M_n = 1.02, [η] = 0.519 dL/g at 35 °C in THF, dn/dc = 0.185 mL/g) provided by Viscotek company.

DVB conversion was determined using the Agilent 6890N gas chromatograph, equipped with an FID detector using a wide-bore capillary column (HP5, 30 m x 0.32 mm x 0.25 µm, J and W Scientific). Injector and detector were kept constant at 280 and 285 °C, respectively.

FT-IR spectra were recorded on a Perkin Elmer Spectrum One FT-IR Spectrometer. Differential scanning calorimetry (DSC) analyses were performed with Perkin Elmer Jade DSC at a heating rate of 10 °C/min under nitrogen atmosphere. All data were collected from a second heating cycle and the glass transition temperatures (T_g) were calculated as a midpoint of thermogram. Thermogravimetric data was obtained using a Thermogravimetric Analyzer Perkin Elmer Pyris 1 between 30–900 °C, under nitrogen, with a scan rate of 10 °C/min. The proton conductivity of membranes was determined by four-probe electrode method using BT-512 BekkTech membrane test system at 100 % relative humidity (RH) at 80 °C.

Morphologies of the membranes were investigated on a scanning electron microscope (SEM) (JEOL 6335F). The SEM analysis was operated at 20 kV accelerating voltage.

Ion Exchange Capacity (IEC)

Ion exchange capacity of multiarm star ionomers were determined by titration method: 0.1-0.2 g. of dried sulfonated polymer were dissolved in 50 mL DMAc and titrated with a 0.1 N standardized NaOH solution diluted five times with absolute methanol to a phenolphthalein endpoint. IEC values for sulfonated polymers were calculated according to eq. 1:

$$\mathrm{IEC} = \frac{V_{NaOH} \times N_{NaOH} \times F_{NaOH}}{W_p} \quad (1)$$

where V_{NaOH} is titrated volume of NaOH solution (L), N_{NaOH} is the normality of NaOH solution and W_p is the weight of dried polymer.

Water uptake

Membranes were conditioned at 105 °C for 1 hour and then at 50 °C for 24 h in an oven. The membranes were cooled to room temperature in a desiccator, immediately weighed and then soaked in deionized water at room temperature for 24 h. Then the membranes were removed, gently wiped with tissue paper, weighed immediately. The water uptake value was calculated according to eq. 2:

$$\mathrm{WU}(\%) = 100 \times \frac{W_{wet} - W_{dry}}{W_{dry}} \quad (2)$$

where W_{dry} and W_{wet} are the weights of dry and wet membranes, respectively.

Oxidative stability

The oxidative stability of membrane was tested by soaking the film in Fenton's reagent (3 % H_2O_2 aqueous solution containing 4 ppm of $FeSO_4$) at 68 °C. The oxidative stability was evaluated by measuring the rupture time of the membranes.

Results and discussion

Multiarm star blok copolymers of PFPMA and PS that served as precursors to the well-defined star ionomers were synthesized according to the previously published procedure (42) by a combination of atom transfer radical polymerization (ATRP) and Diels–Alder click reaction based on so-called "arm first" method as outlined in Figure 1. First, PS arms, with a narrow molecular weight distribution, were synthesized by ATRP of St using CuBr/PMDETA as a catalyst and 9-anthyryl methyl 2-bromo-2-methyl propanoate (**1**) as a functional initiator at 110 °C. Three PS-anthracene with various molecular weights were prepared for the synthesis of multiarm star polymer with different arm numbers.

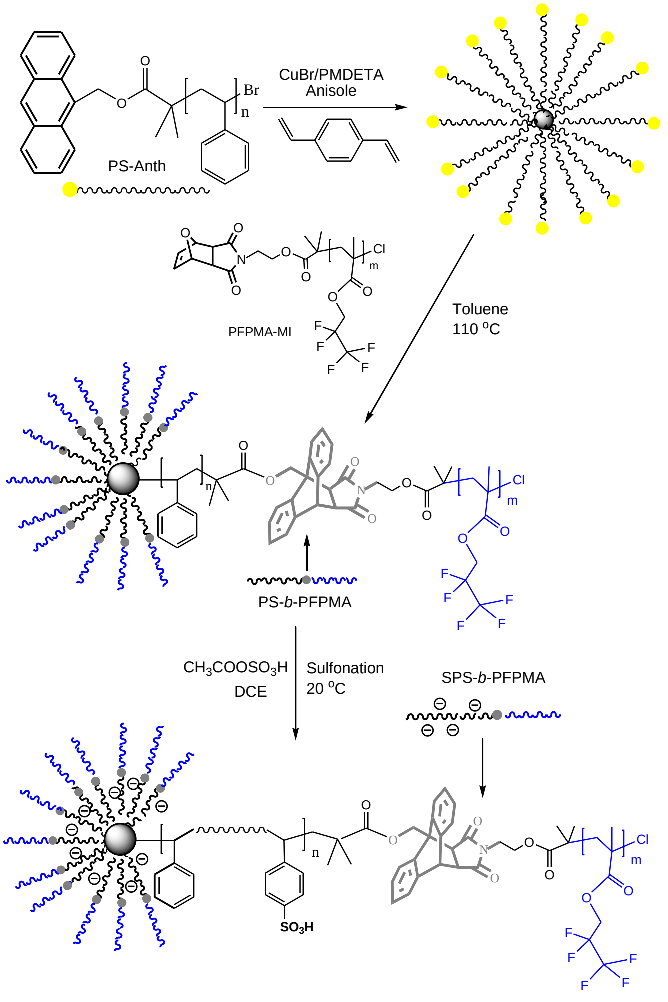

Figure 1. Schematic representation of the synthesis of multiarm star block copolymer: PS-*b*-PFPMA (PS: black, PFPMA: blue) and its sulfonation.

Independently, α-furan protected maleimide end-functionalized PFPMA (PFPMA-MI) was prepared by ATRP of FPMA in the presence of **2** as initiator, $CuCl/CuCl_2$/PMDETA as a catalyst system at 70 °C in toluene. Maleimide functionalities were protected as they can contribute to the free copolymerization with FPMA.

Up to now, the synthesis of PFPMA has been accomplished by free radical polymerization (43-45). There was no report on controlled polymerization of FPMA. As it was previously stated, the bromine terminal group of acrylate can be converted to chlorine soon after the polymerization of methyl methacrylate started where CuCl was used as the Cu(I) species. Thus, the halogen exchange enhances the rate of initiation over the rate of propagation (46). In the case of ATRP of FPMA, both the mix halogen system and additional deactivator ($CuCl_2$) were used for the ease of control in the polymerization. Due to the low refractive index values of fluorinated compounds, the GPC analysis of the synthesized PFPMA was performed in the negative polarity. The molecular weight distributions of all precursors were low and their GPC traces were monomodal (Figure 2).

Anthracene-end functionalized polystyrene-*block*-poly(divinyl benzene) star copolymer was prepared using PS-anthracene as macroinitiator and divinyl benzene as cross-linker in ATRP condition at 110 °C. As it was previously stated, soluble multiarm star polymer could be readily obtained when a suitable molar ratio of DVB to macroinitiator (i.e., 15) was utilized (47,48). The polymerization time varied to adjust the different arm numbers in the resulting multiarm star polymers. The unreacted PS-anthracene was removed by dissolving the polymer in THF and then precipitating in methanol/diethyl ether mixture (1/1 v/v). The conventional SEC traces of the purified multiarm star polymer and its precursor (PS-Anth) were shown in Figure 2.

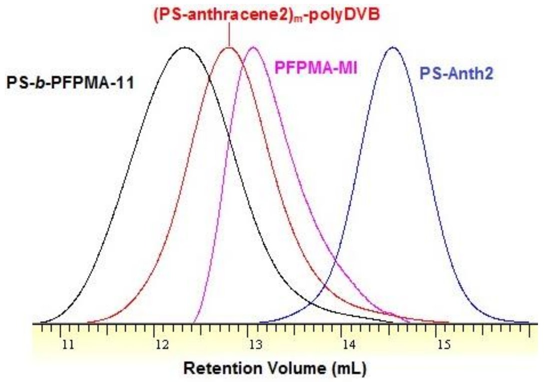

Figure 2. The evolution of SEC traces 11-arm PS-*b*-PFPMA star block copolymer and its precursors

A clear shift to the higher molecular weight region was observed indicating the formation of multiarm star polymer with high efficiency. The absolute molecular weights of star polymers were calculated using triple-detector (refractive index (RI), light scattering (LS) and differential viscometer) SEC (TD-SEC) instrument. The refractive index increment (dn/dc) of multiarm $(\text{PS-anthracene})_m$-*b*-polyDVB star copolymer was measured by TD-SEC instrument and found to be 0.185 mL/g in THF at 35 °C which was equal to that of linear PS. The weight average arm numbers (f) of multiarm $(\text{PS-anthracene})_m$-*b*-polyDVB star polymers were calculated according to the published work (42) using equation 3 based on the absolute molecular weights (M_w) of multiarm star polymer.

$$f = \frac{WF_{arm} \times M_{w,star}}{M_{w,arm}}$$
$$= \frac{M_{w,star}}{M_{w,arm} + M_{DVB} \times conv_{DVB} \times [\mathrm{DVB}]/[\mathrm{PS-Anth}]} \quad (3)$$

where WF_{arm} is the weight fraction of PS arm in the star polymer, $M_{w,star}$ and $M_{w,arm}$ are the absolute molecular weights of the $(\text{PS-anthracene})_m$-polyDVB star and PS-anthracene arm, respectively, obtained from TD-SEC instrument introducing the predetermined dn/dc value of PS to OmniSEC software, M_{DVB} is the molecular weight of DVB, [DVB]/[PS-Anth] is a feed molar ratio of the DVB to PS-Anth before cross-linking polymerization. The conversion of DVB ($Conv_{DVB}$) was determined by GC. Thus, the weight average arm numbers (*f*) of per molecule $(\text{PS-anthracene})_m$-polyDVB were calculated to be 6, 11 and 15. The molecular weight values (M_n, M_w, M_p) of multiarm star PS obtained using conventional SEC and TD-SEC were given in Table 1. From Table 1 it can be seen that M_n values of multiarm star PS determined by conventional SEC are considerably smaller than that of the absolute molecular weight data, which points to the expected compact structure of the multiarm stars.

As previously reported by Tunca and coworkers (42), the combined retro-DA and "DA click reaction" utilizing polymers with antagonist functional groups lead to the formation of well-defined multiarm star block copolymers with low degree of heterogeneity. The obtained anthracene-end functionalized $(\text{PS})_m$-polyDVB ($(\text{PS-anthracene})_m$-polyDVB) multiarm star copolymer was then reacted with PFPMA-MI to give multiarm star block copolymer via Diels-Alder click reaction. Deprotection of maleimide-functionalized polymer (retro-DA) was carried out in situ during Diels-Alder-"click reaction"- by heating $(\text{PS-anthracene})_m$-polyDVB multiarm star polymers with maleimide end functional PFPMA (PFPMA-MI) precursor in toluene at 110 °C. PFPMA-MI was used in a slight excess (1.2 equiv.) with respect to the $(\text{PS-anthracene})_m$-polyDVB multiarm star copolymer. The respective multiarm polystyrene-*block*-poly(2,2,3,3,3-pentafluoropropyl methacrylate), (PS-*b*-PFPMA) star block copolymers were obtained with quantitative yields without need for an additional purification step. The byproduct (furan) and excess PFPMA-MI were removed by precipitating the polymer mixture in methanol at room temperature. Figure 2 shows the evolution of SEC traces of the linear PS-anthracene and PFPMA-MI precursors and 11-arm $(\text{PS-anthracene})_m$-polyDVB star copolymer and 11-arm PS-*b*-

PFPMA star block copolymer. The clear shift for (PS-anthracene)$_m$-polyDVB multiarm star copolymer to the higher molecular weight region revealed that the formation of multiarm PS-*b*-PFPMA star block copolymer occurred by efficient Diels-Alder reaction. Since the calculation of dn/dc value of PFPMA-MI could not be possible using TD-SEC in THF mobile phase due to low refractive index value of PFPMA, the absolute molecular weights of multiarm star block copolymers were not calculated.

The structure of multiarm PS-*b*-PFPMA star block copolymers was characterized by ^{1}H-NMR (Figure 3). The characteristic signal of anthracene aromatic protons between 7.4 and 8.5 ppm completely disappeared and the new signals corresponding to CH_2 protons adjacent to the anthracene ring and a bridgehead proton of the cycloadduct CH, appeared at 5.3 and 4.7 ppm, respectively. The signals at 4.4 and 3.7 ppm are assignable to the OCH_2 of PFPMA backbone and CH_2 protons adjacent to the (OCH_2CH$_2$N), respectively. Moreover, the resonances at 3.5 (OCH$_2$CH_2N) and 3.3 ppm (CHCH protons of the imide ring) were primarily observed. The mole fractions of PS and PFPMA blocks in multiarm star block copolymers were calculated from ^{1}H-NMR comparing the related backbone protons and tabulated in Table 2. In order to investigate the influence of fluorinated backbone on the ionomer properties, a set of multiarm star block copolymers with different PFPMA content were synthesized (Table 2).

The sulfonic acid moiety was introduced to multiarm PS-*b*-PFPMA star block copolymers via sulfonation (Figure 1). Sulfonation of phenyl ring of PS block using acetyl sulfate was carried out according to the method of Makowski *et al.* (40, 41) but with slight modification. A relatively low reaction temperature (20 °C) was utilized to control the sulfonation degree with ease and to obtain soluble multiarm star ionomers. The insoluble ionomers were obtained when the sulfonation was conducted at 30 °C. It was anticipated that sulfonation of PS block of multiarm star block copolymers could be carried out to desirable conversion using acetyl sulfate without sulfonation of the aromatic rings within the DVB core due to the poor solubility of acetyl sulfate in hydrocarbons (49). Thus, the sulfonation agent was not expected to penetrate into the vicinity of the star core where the high concentration of PS and PFPMA chain segments is considered. The ion exchange capacity (IEC) of ionomers was determined by titration of sulfonated multiarm star block copolymers with appropriate amount of base (sodium hydroxide solution).

Table 1. The characterization of anthracene-end functionalized PS and multiarm (PS-anthracene)$_m$-polyDVB star polymer

Polymer	SEC[b]						TD-SEC[d]				
	M_n	M_w (g/mol)	M_p	*Đ*	*Time (h)*	*Conv.*[c] *(%)*	M_n	M_w (g/mol)	M_p	[η] (dL.g^{-1})	*f*[e]
PS-Anth1	6400	7150	6700	1.12	0.6	25	8200	9100	8250	0.08	-
PS-Anth2	5000	5650	5400	1.13	0.5	21	6500	7100	6600	0.07	-
PS-Anth3	9000	10000	9400	1.11	0.5	21	10600	11650	10800	0.08	-
(PS-anthracene1)$_m$-polyDVB[a]	35150	53600	65550	1.52	11.0	84	105330	156000	169700	0.14	15
(PS-anthracene2)$_m$-polyDVB[a]	29100	40000	36700	1.38	12.5	72	70300	93700	81100	0.13	11
(PS-anthracene3)$_m$-polyDVB[a]	35650	50200	50150	1.41	13.5	58	56600	79800	75900	0.12	6

[a] [DVB]/15:[PS-Br]:[CuBr]:[PMDETA]:0.023 M in anisole at 110 °C.

[b] Molecular weights were calculated by the aid of linear PS standards.

[c] Conversions were calculated gravimetrically. DVB conversions were calculated by GC.

[d] Weight average molecular weights of star polymers were calculated using Triple Detection SEC (TD-SEC) (Agilent model, RI, dual laser light scattering (DLLS) (λ= 670 nm, 90◦ ve 7◦) and differential pressure viscometer at 35°.

[e] Number of arms in multi arm star polymer, calculated according to eq 3. [f] dn/dc value of (PS-anthracene)$_m$-*b*-polyDVB star copolymers was measured by TD-SEC and found to be 0.185 mL/g in THF at 35 °C which was equal to that of linear PS.

Table 2. The characterization of multiarm star block copolymers

Multiarm star block copolymer	[(PS-anthraceneX)$_m$-polyDVB]$_0$:[PFPMA-MI]$_o$	Time (h)	$M_{n,SEC}$[a]	*Đ*[a]	PFPMA[b] (mole %)
PS-*b*-PFPMA-15	1:22.5	62	85400	1.39	47.0
PS-*b*-PFPMA-11	1:16.5	71	47000	1.66	33.6
PS-*b*-PFPMA-6	1:9.0	63	53600	1.61	27.0

[a] Molecular weights were calculated by the aid of linear PS standards.

[b] Calculated by ^{1}H-NMR spectroscopy.

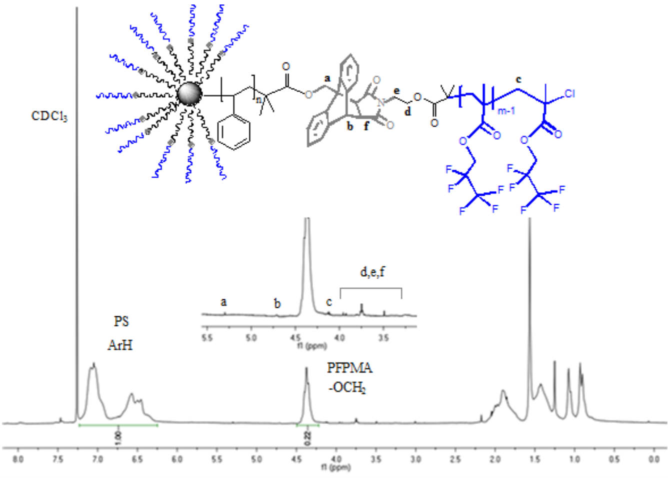

Figure 3. ^{1}H NMR spectrum of 11-arm PS-*b*-PFPMA star block copolymer in $CDCl_3$.

The characteristics of sulfonated multiarm PS-*b*-PFPMA star block copolymers, (SPS-*b*-PFPMA) used in this study are listed in Table 3. Sample SPS-PFPMA-6(1.3), for example, is the sulfonated 6-arm PS-*b*-PFPMA star block copolymer with 1.3 mmol/g IEC.

Ionomers with different sulfonic acid content were prepared by changing the sulfonation time. Multiarm SPS-*b*-PFPMA star block copolymers were sulfonated to different sulfonation levels ranging from 0.67 to 1.68 mmol/g. Anthracene end functionalized (PS-anthracene1)$_m$-polyDVB multiarm star copolymer series were also sulfonated for comparison. The sulfonated polymers were readily soluble in polar aprotic solvents such as *N*,*N*-Dimethylformamide (DMF), *N*,*N*-Dimethylacetamide (DMAc), *N*-Methylpyrrolidone (NMP), and dimethyl sulfoxide (DMSO). The ion exchange capacity, which is the miliequivalents of SO_3H^+ per weight of the dry polymer, is plotted against sulfonation time for the sulfonation of multiarm star and star block ionomers (Figure 4).

As can be seen in Figure 4, IEC values of multiarm star ionomers increased with increasing sulfonation time as expected. Depending on the arm number and the composition of the multiarm star ionomer, the evolution of IEC shows different trends. Higher IEC values were obtained for 15-arm sulfonated (PS-anthracene)$_m$-polyDVB star copolymer than those of fluorinated 15-arm SPS-*b*-PFPMA star block ionomers. This is expected because longer fluorinated block should make the penetration of sulfonating agent to the vicinity of the PS block difficult, resulting the lower IEC values. Moreover, DCE is probably a better solvent for PS than for PFPMA. For PS-*b*-PFPMA-11, we conducted sulfonation reactions with reaction times of 15 h or longer. For reaction times larger than 20 h, desulfonation process became dominant and the measured IEC values were much lower (of the order of 0.4 mmol/g). We have been investigating the possible reasons of the observed desulfonation and these data were not included in Figure 4. Within the series of star block ionomers possessing different arm numbers, 6-arm SPS-*b*-PFPMA star block ionomers was sulfonated to higher sulfonation levels. It can be attributed to the lower concentration of PS and PFPMA chain segments of the 6-arm star core which make the penetration of sulfonation agent to the vicinity of the PS block easier when compared to 15- and 11-arm star block ionomers.

FTIR spectroscopy was used to confirm the partial sulfonation of the styrene groups of multiarm star block copolymers (Figure 5). The appearance of characteristic peaks due to symmetric stretching of SO_3^- at 1033 cm^{-1} and in-plane bending of para-substituted phenyl ring at 1006 cm^{-1} confirm introduction of sulfonic groups (50, 51). The characteristics peaks from the PFPMA component at 1752 cm^{-1} (C=O stretching), 2852 and 2926 cm^{-1} (C-H stretching), 1105-1260 cm^{-1} (C-F stretching) and 1186 cm^{-1} (CF_3), were also assigned.

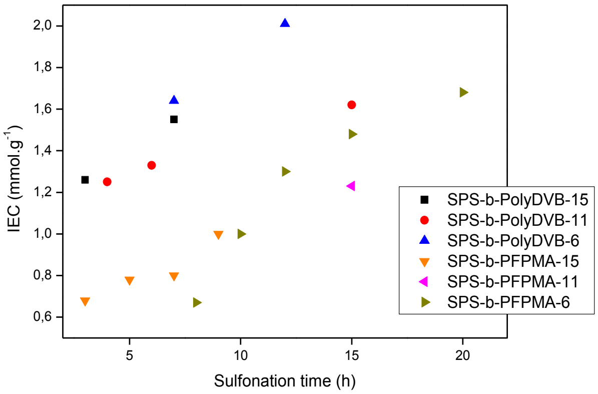

Figure 4. Evolution of IEC with sulfonation time.

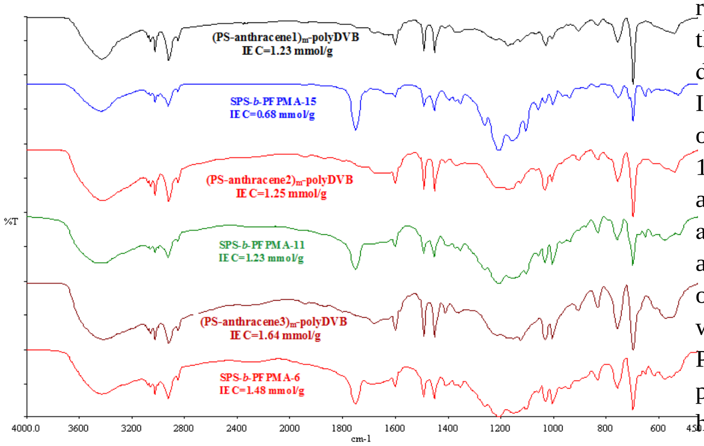

Figure 5. FTIR spectra of selected multiarm (PS-anthracene)$_m$-polyDVB star block copolymer ionomers and SPS-*b*-PFPMA star block ionomers with different IECs.

Incorporation of sulfonyl groups has been also confirmed by ^{1}H-NMR analysis. ^{1}H-NMR spectrum of SPS-*b*-PFPMA-6(1.48) is shown in Figure 6. Besides the characteristic peaks corresponding to PS and PFPMA segments, a new signal corresponding to aromatic protons adjacent to -SO$_3$H group appeared at around 7.5 ppm.

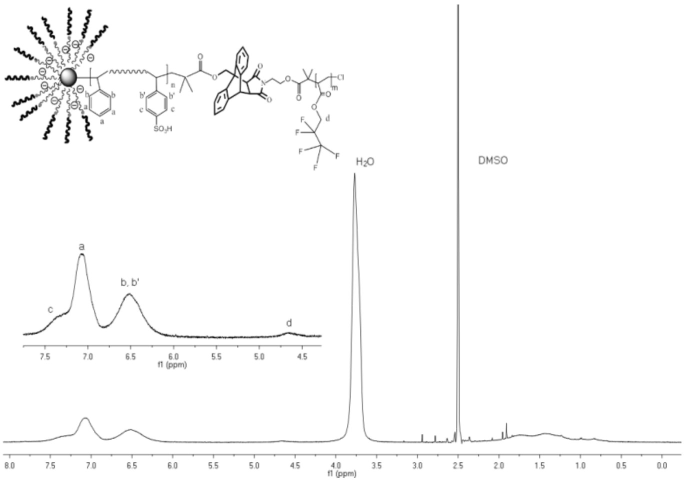

Figure 6. ^{1}H-NMR spectrum of SPS-*b*-PFPMA-6(1.48) in DMSO-d6.

Thermal Analysis

The thermal stability of the multiarm stars and their ionomers was investigated by TGA. TGA curves for the 6-, 11-, and 15-arm PS-*b*-PFPMA star block copolymer and their corresponding SPS-*b*-PFPMA star block ionomers prepared in this work are shown in Figure 7 and Figure 8 for different IECs. PS-*b*-PFPMA star block copolymer series reveals a three-step thermal decomposition. The first step occurs below 300 °C, followed by the second major decomposition step at 370 °C. The two steps involve the depolymerization of PFPMA, leading to chain scission. The last weight loss stage around 400 °C is due to the polymer (PS) backbone degradation. The decomposition of the star ionomers was produced also in three stages; the first one consists of small transition in the 50-180 °C range that can be attributed to the presence of moisture due to the hygroscopic nature of sulfonated PS blocks. The percentage decrease in mass due to water loss (up to 180 °C) increases with IEC. The higher moisture content observed for the membranes of SPS-*b*-PFPMA-6 (IEC=1.68 mmol.g^{-1}) and SPS-*b*-PFPMA-11 (IEC=1.23 mmol.g^{-1}) was associated with higher sulfonic acid content of the membranes. Second transition was observed around 300 °C due to the decomposition of sulfonic acid groups and depolymerization of PFPMA. Finally, main chain scission occured around 400 °C. The higher decomposition temperature was observed for sulfonated star block copolymers than PS-*b*-PFPMA star block copolymer, which is consistent with previous reports indicating that the sulfonated PS blocks show higher thermal stability than its pristine polymer (13).

Glass transition temperatures (T_g) of multiarm PS-*b*-PFPMA star block copolymers and their ionomers possessing different IECs are given in Table 3. 15-arm multiarm star block copolymer shows only one T_g at around 65 °C corresponding to PFPMA component. This was attributed to restricted segmental motion of PS/SPS segment due to the fluorinated block at the periphery of multiarm star, especially higher number of arms is considered.

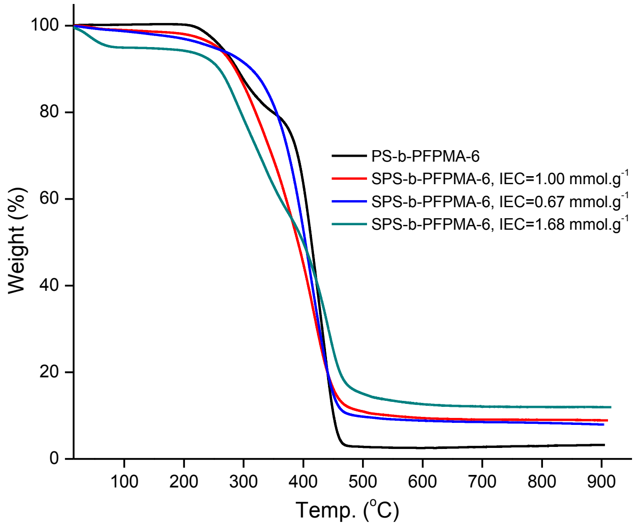

Figure 7. TGA curves of 6-arm SPS-*b*-PFPMA with different IECs.

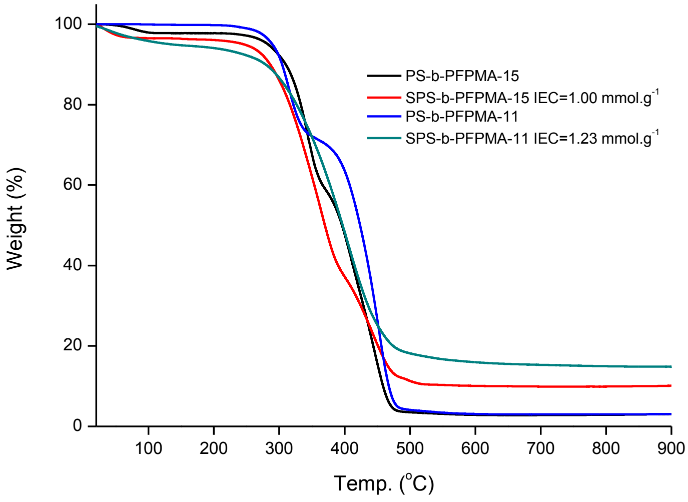

Figure 8. Comparison of TGA curves of 11-arm and 15-arm SPS-*b*-PFPMA with different IECs.

For the 6-arm and 11-arm star block ionomers mostly two T_g's are observed: one due to the fluoropolymer segment which occurs at around 65 °C, and the other due to the partially sulfonated polystyrene, which varies in temperature between 117 (IEC=0.67 mmol/g) and 157.8 °C (IEC=2.01 mmol/g). The unsulfonated star block copolymers with 6- and 11-arm exhibits in most cases T_g's of 65 and 110 °C for PFPMA and PS, respectively. The sulfonation of PS block does not show any effect on the T_g of the fluorinated block. However, all the ionomer samples show T_g of the PS block higher than that of unsulfonated stars due to the bulkiness of the sulfonate group and due to the ionomeric effect (52). As the ion exchange capacity increases, the T_g of the sulfonated PS segment increases regardless of arm number, molecular weight and composition of sulfonated block copolymers.

Table 3. T_g's of multiarm star/star block (co)polymers and their ionomers.

Multiarm star polymer	**IEC (mmol.g^{-1})**	**$T_{g,PS}$[a]**	**$T_{g,PFPMA}$[a]**
(PS-anthracene1)$_m$-polyDVB-15	-	115.5	-
(SPS-anthracene1)$_m$-polyDVB-15	1.26	132.2	-
	1.55	154.1	
PS-*b*-PFPMA-15	-	-	46.0
SPS-*b*-PFPMA-15	0.68	-	64.5
	1.00	-	63.6
(PS-anthracene2)$_m$-polyDVB-11	-	115.2	-
(SPS-anthracene2)$_m$-polyDVB-11	1.25	134.6	-
	1.62	n.d.[b]	-
(PS-anthracene3)$_m$-polyDVB-6	-	109.0	-
(SPS-anthracene3)$_m$-polyDVB-6	1.64	156.5	-
	2.01	157.8	-
PS-*b*-PFPMA-6	-	109.0	-
SPS-*b*-PFPMA-6	0.67	117.9	67.6
	1.00	143.5	62.0
	1.30	142.8	64.7
	1.48	152.1	69.8
	1.68	n.d.[b]	n.d.[b]

[a] Measured under N_2 at 10 °C min.$^{-1}$ [b] n.d.: not determined because of high ion exchange capacity value.

Multiarm star ionomer membranes and blend membranes

The solution cast membranes of 11- and 15-arm star and star block ionomers exhibited poor mechanical properties, to some extent, in the humidified state and became brittle when dried. This is attributed to low segmental mobility of partially sulfonated PS block due to dense core structure of ionomeric star molecule and high density of hydrophobic PFPMA block at the periphery. This is consistent with other reports of hyperbranched polymeric based proton exchange and gas separation membranes (53, 54).

6-arm SPS-*b*-PFPMA (27 mol % PFPMA) ionomer having an IEC of 1.00 mmol/g give tough and flexible membrane both in its dry and hydrated states. As it is known, star-branched polymers the segment density near the center of the star is larger the larger the number of arms is. It can be concluded that less restricted segmental motion of sulfonated PS block enhance the ductility of the produced membrane.

To improve the flexibility of the membranes, blend membranes of multiarm star ionomers and sulfonated poly(2,6-dimethyl-1,4-phenylene oxide) (PPO) were prepared. It has been known that PPO is well miscible with PS due to phenylene phenylene interaction (55). Sulfonated PPO (SPPO) (56,57) with good mechanical and chemical stability and SPPO blends such as SPPO/SPS, SPPO/polybenzimidazole (PBI) (58,59) are extensively used as PEM materials. It was well established that the optimal phase separations between hydrophilic and hydrophobic domains can be controlled by blending the partially sulfonated PS and the partially sulfonated PPO together through effective hydrogen bonding when the membranes are their hydrated states. PPO was sulfonated using acetyl sulfate in chloroform according to the published procedure. The multiarm star ionomer blend membranes were prepared, using SPPO with 1.34 mmol/g IEC and 2.41 mmol IEC. A concentration of 40 wt. % SPPO was found to give enough mechanical stability to multiarm star/star block ionomer membranes for proton conductivity analysis as a function of IEC as shown in Figure 9.

Water uptake and proton conductivity

Water uptake is typically a function of sulfonic acid content of proton conducting polymers. Generally, the water plays a critical role in PEMs and is regarded as a transportation medium of protons that enable high proton conductivity. The water uptake of 6-arm multiarm star ionomer/SPPO blend membranes was measured and is listed in Table 4. As can be seen from Table 4, with increasing IEC of blend membranes from 0.86 to 1.37 mmol/g, the water uptakes increased from 8.3 % to 32.4 %. At an IEC value of 1.34 mmol/g, SPPO was considerably less densely sulfonated than the sulfonated multiarm star block copolymers at similar IEC values. The water uptakes of blend membranes prepared with the SPPO (1.34 mmol/g) and 6-arm star block ionomer (1.30 and 1.48 mmol/g) are drastically higher than that of pristine SPPO (WU=7.7 %), which indicates that the star ionomer can absorb and hold a lot of water because of the high density of sulfonic acid groups at the core. This result confirms that the multiarm star block structure with hydrophilic SPS segments surrounded by hydrophobic fluorinated segments tends to enhance the water-holding property. This is consistent with other star ionomer membrane study based on star-shaped sulfonated block copoly(ether ketone)s (60).

The proton conductivities of multiarm star ionomer and their blend membranes possessing different IEC values measured at 25 and 80 °C and relative humidity (RH) of 100 % with Becktech Membrane conductivity test system (Table 4). 11-arm SPS-*b*-PFPMA (IEC=1.23 mmol/g)/SPPO (IEC=2.41 mmol/g) blend membrane shows 20.3 mS/cm conductivity which is higher than that of pristine SPPO (13.7 mS/cm) (Table 4). 15-arm star/SPPO blend membrane is too brittle for the conductivity measurement.

Table 4. Proton conductivities and oxidative stabilities 6-arm and 11-arm star block ionomer, their SPPO blend membranes and SPPOs.

Membrane	**IEC$_p$^{a} (mmol.g^{-1})**	**σ $_{25°C}$ (mS.cm^{-1})**	**σ $_{80°C}$ (mS.cm^{-1})**	**WU (%)**	**Rupture time in Fenton test^b (h)**
SPS-*b*-PFPMA-6	1.00	8.59	19.37	-	2
SPS-*b*-PFPMA6 /SPPO(1.34)(40wt.%)	0.86	8.08	15.62	8.30	23
	1.30	15.75	42.50	30.34	17
	1.37	12.71	31.63	32.40	5
	1.48	5.53	9.25	-	6
	1.68	2.38	7.69	-	3
SPPO(1.34)	1.34	1.80	3.82	7.70	22
SPS-*b*-PFPMA11 /SPPO(2.41)(80wt.%)	1.23	-	20.3	-	52
SPPO(2.41)	2.41	-	13.7	-	2

^{a}IEC$_p$: IEC of sulfonated polymer, ^{b}Rupture time in Fenton reagent at 68 °C.

A series of blend membranes were prepared using 6-arm SPS-*b*-PFPMA possessing different IECs and SPPO having 1.34 mmol/g IEC. As seen in Table 4, all the blend membranes had a significantly higher conductivity than SPPO(1.34) at similar IECs. Partially sulfonated PPO can be considered to be random copolymers of PPO and sulfonated PPO that sulfonic acid groups disperse throughout the polymer backbone which leads to a quite low water uptake and inability to form an efficient pathway for proton conduction. In a series of 6-arm star block ionomer/SPPO blend membranes, the conductivities are increased with increasing IEC from 0.86 to 1.30 mmol/g because of improved ion contents of the membranes and thereafter levels off. As seen in Figure 9, a further increase in IEC (1.48 and 1.68 mmol/g) leads to a decreased conductivity. This is attributed to reduced proton concentrations as a result of increased water uptake, as similar phenomena have been observed in other ionic polymers (61-64).

The highest proton conductivity of 42.5 mS/cm was obtained for the blend membrane of 6-arm SPS-*b*-PFPMA with 1.30 mmol/g IEC at 80 °C. The high proton conductivity is thought to be originated from the optimum phase segregated morphology of partially fluorinated star block copolymer structure and high density of sulfonic acid groups at the core. The fluoropolymer block segments induce formation of connected ion channels which results in enhanced proton transport.

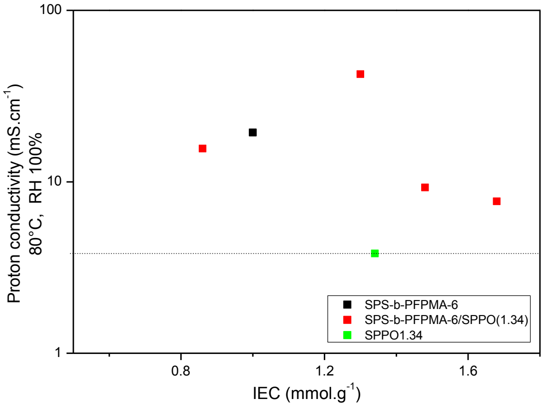

Figure 9. IEC versus proton conductivity for 6-arm star block ionomer, its blend membranes and SPPO(1.34)

Oxidative stability

The oxidative stability of the blend membranes and SPPO was evaluated in Fenton's reagent at 68 °C as an accelerated test. The time of rupture of membranes were collected and summarized in Table 4. SPPO membranes with 2.41 mmol/g IEC ruptured in Fenton's reagent in only 2 hours. A decrease in oxidative stability with an increase in the IEC value of the polymer is generally observed. 11-arm SPS-*b*-PFPMA (IEC=1.23 mmol/g) blend membrane showed higher oxidative stability than SPPO membrane (IEC= 2.41 mmol/g). The higher oxidative stability of star ionomer may be derived from the hydrophobic segments at the periphery. 6-arm SPS-*b*-PFPMA blend membrane series showed comparable oxidative stability with SPPO membrane having 1.34 mmol/g IEC (Table 4). 11-arm blend membrane has a better oxidative stability against Fenton's reagent compared to 6-arm blend membrane series with similar IEC values which indicate that the high density of fluorinated segment can effectively improve the oxidative stability.

Morphologies of Membranes

The morphology of 6-, 11- and 15-arm sulfonated (PS-anthracene)$_m$-*b*-polyDVB star copolymer and SPS-*b*-PFPMA star block ionomer membranes has previously been characterized by Small Angle X-ray Scattering (SAXS) (65) SPS membranes showed well-defined ionomer peaks corresponding to an average distance of ~7 nm between the ionic clusters. In the case of SPS-*b*-PFPMA membranes, in addition to ionomer peak, a second more intense peak corresponding to a spacing of ~25 nm was observed due to the phase separation of SPS block at the core and PFPMA block at corona. SEM analysis of the top surface of membranes did not show any texture, but a rather smooth surface. Cross-sectional SEM analysis of the membranes was performed. Figure 10a and

Figure 10b show the SEM micrographs of 15-arm sulfonated (PS-anthracene)$_m$-*b*-polyDVB star copolymer ionomer membranes having IEC=1.26 mmol/g and 1.55 mmol/g, respectively. Granular features having sizes between 40 and 70 nm were observed for both membranes. Similar morphology was also observed for SPS-*b*-PFPMA star block ionomer membranes as shown in Figure 10c. The average size of phase separated 6-arm SPS-*b*-PFPMA was estimated to be ~24-29 nm while that of 15-arm SPS-*b*-PFPMA was ~32-37 nm as determined by SAXS (65). The size of the granules (50-70 nm) seen in SEM pictures of Figure 10a-c are larger than the size of the multiarm star molecules which indicates that each granule contains more than one multiarm star molecules. The granular morphology does not prevent the formation of ionic clusters as well-defined ionomer peaks were observed by SAXS for all membranes.

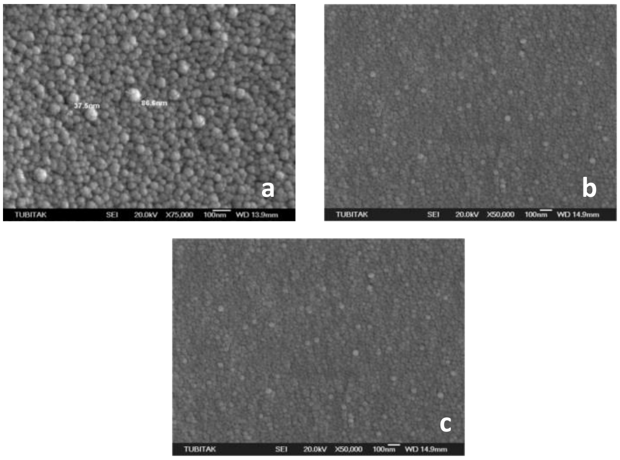

Figure 10. Cross-sectional SEM micrographs of membranes of (a) (SPS-anthracene1)$_m$-polyDVB-15, IEC = 1.26 mmol.g^{-1}, (b) (SPS-anthracene1)$_m$-polyDVB-15, IEC = 1.55 mmol.g^{-1}, (c) SPS-*b*-PFPMA-15, IEC = 1.00 mmol.g^{-1}.

Conclusions

Multiarm star block copolymers with sulfonated hydrophilic core and hydrophobic fluorinated periphery have been tailored and prepared as proton conducting membrane materials. Thermal characterization by DSC confirmed the microphase separated morphology of the star ionomers with a hydrophobic PFPMA phase and a partially sulfonated PS phase. The solution cast membranes of 11- and 15-arm star and star block ionomers exhibited poor mechanical properties compared to 6-arm star ionomers. The blend membranes of star ionomers with sulfonated SPPO give though and flexible membranes mostly in their hydrated states. As expected, the proton conductivity of the star ionomer membranes depended on the IEC and the level of the connectivity of the ionic phases resulting from the morphology. At a given IEC, the proton conductivity of under fully humidified conditions of all the star ionomer blend membranes exceeded that of sulfonated PPO membrane which demonstrated that the phase segregated morphology of partially fluorinated star block copolymer structure and high density of sulfonic acid groups at the core of the star polymer has positive impact on the proton conductivity. Thus, the work has shown that it is possible to prepare proton exchange membranes with well-controlled morphology and reasonable proton conductivity by using star block copolymers with a sulfonated core having fluorinated hydrophobic periphery.

Acknowledgements

The authors thank TUBITAK (The Scientific and Technological Research Council of Turkey) for financial support (TBAG-109T798).

Notes and references

[a] Chemistry Institute, TUBITAK Marmara Research Center, Gebze 41470, Kocaeli, TURKEY,
[b] Department of Chemistry, Istanbul Technical University, Maslak 34469, Istanbul, TURKEY
[c] Department of Chemistry, Koç University, Sarıyer 34450, Istanbul, TURKEY

1. G.G Scherer, *Advances in Polymer Science*, 2008.
2. M.A. Hickner, H. Ghassemi, Y.S. Kim, B.R. Einsla and J.E. McGrath, *Chem. Rev*., 2004, **104**, 4587.
3. H. Zhang, P.K. Shen, *Chem. Rev*., 2012, **112**, 2780.
4. S.J. Sondheimer, N.J. Bunce, C.A. Fyfe, *J. Macromol. Sci., Rev. Macromol. Chem. Phys*, 1985, **C26**, 353.
5. Y. Shao, G. Yin, Z. Wang, Y. Gao, *J. Power Sources*, 2007, **167**, 235.
6. Y. Yang, S. Holdcroft, *Fuel Cells*, 2005, **5,** 171.
7. B. Smitha, S. Sridhar and A.A. Khan. *J. Membr. Sci.*, 2003, **225**, 63.
8. L.W. Zhang, S.R. Chae, Z. Hendren, J.S. Park and Mr. R. Wiesner, *Chem. Eng. J*., 2012, **204**, 87.
9. Y. A. Elabd, M. A. Hickner, *Macromolecules*, 2011, **44**, 1.
10. A. Nacher, P. Escribano, C. Del Rio, A. Rodriguez and J.L. Acosta, *J. Polym. Sci., Part A: Polym. Chem.*, 2003, **41**, 2809.
11. P.H. Vargantwar, M.C. Brannock, K. Tauer and R.J. Spontak. *J. Mater. Chem. A.*, 2013, **1**, 3430.
12. E.M.W. Tsang, Z. Zhang, Z. Shi, T. Soboleva and S. Holdcroft. *J. Am. Chem. Soc.*, 2007, **129**, 15106.
13. R.A. Weiss, A. Sen, C.L. Willis and L.A. Pottick, *Polymer*, 1991, **32**, 1867.
14. J. Kima, B. Kima and B. Jung, *J. Membr. Sci.*, 2002, **207**, 129.
15. Y.A. Elabd, E. Napadensky, C.W. Walker and K.I. Winey, *Macromolecules*, 2006, **39**, 399.
16. Y. A. Elabd, E. Napadensky, J. M. Sloan, D. M. Crawford and C. W. Walker, *J. Membr. Sci.*, 2003, **217**, 227.
17. Y. A. Elabd, C. W Walker and F. L. Beyer, *J. Membr. Sci.*, 2004, **231**, 181.
18. Y. A. Elabd, E. Napadensky, *Polymer*, 2004, **45**, 3037.
19. D. Gromadzki, P. Cernoch, M. Janata, V. Kudela, F. Nallet, O. Diat, and P.S Tepanek, *Eur. Polym. J.*, 2006, **42**, 2486.
20. B. Loppinet, G. Gebel and C.E. Williams, *J. Phys. Chem. B.*, 1997, **101**, 1884.

21. M. J. Park, N. P. Balsara, *Macromolecules*, 2010, **43**, 292.
22. S. J. Lee, M. J. Park, *Soft Matter*, 2011, **7**, 8838.
23. T. Erdogan, E. Erdal Unveren, T. Y. Inan and B. Birkan, *J. Membr. Sci.*, 2009, **344**, 172.
24. W.H. Choi, W.H. Jo, *J. Power Sources*, 2009, **188**, 127.
25. L. Chen, D T. Hallinan, Y. A. Elabd and M.A. Hillmyer, *Macromolecules*, 2009, **42**, 6075.
26. T. Saito, H.D. Moore and M.A. Hickner. 2010, Cilt 43. 599.
27. J. F. Ding, Q. Y. Tang and S. Holdcroft. *Aust. J. Chem.*, 2002, **55**, 461.
28. J. F. Ding, C. Chuy, and S. Holdcroft, *Macromolecules*, **35**, 1348.
29. J.F. Ding, C. Chuy, and S. Holdcroft. *Adv. Funct. Mater.*, 2002, 12, 389.
30. Z. Q. Shi, S. Holdcroft, *Macromolecules*, 2004, **37**, 2084.
31. Z. Q. Shi, S. Holdcroft, *Macromolecules* 2005, **38**, 4193.
32. E.M.W. Tsang, Z. Zhang, Z Shi, T. Soboleva and S. Holdcroft, *J. Am. Chem. Soc.* 2007, **129**, 15106.
33. E. M. W. Tsang, Z. Zhang, A. C. C. Yang, Z. Shi, T. J. Peckham, R. Narimani, B. J. Frisken and S. Holdcroft, *Macromolecules*, 2009, **42**, 9467.
34. E.M.W. Tsang, Z. Zhang, Z. Shi, T. Soboleva, S. Holdcroft, *J. Am. Chem. Soc.*, 2007, **129**, 15106.
35. E. M. W. Tsang, Z. Q. Shi and S. Holdcroft, *Macromolecules*, 2011, **44**, 8845.
36. A. Mokrini, J. L. Acosta, *Polymer*, 2001, **42**, 8817.
37. K. Matsumoto, T. Higashihara and M. Ueda, *Macromolecules*, 2008, **41**, 7560.
38. H. Durmaz, B. Colakoglu, U. Tunca and G. Hizal, *J. Polym. Sci. Part A: Polym. Chem.*, 2006, **44**, 1667.
39. G. Mantovani, F. Lecolley, L. Tao, D. M. Haddleton, J. Clerx, J.J.L. M. Cornellisen and K. Velonia, *J. Am. Chem. Soc*., 2005, **127**, 2966.
40. H.S. Makowski, R.D. Lundberg and G.S. Singhal, US Patent 3,870,841 1975.
41. J. Bock, R.D. Lundberg and H.S. Makowski, US Patent 4,184,988 1980.
42. A. Dag, H. Durmaz, U. Tunca and G. Hizal, *J. Polym. Sci. Part A: Polym. Chem*, 2008, **47**, 178.
43. H. L. Huang, S. H. Goh, A. T. S. Wee Polymer, 2002, **43**, 2861.
44. M.. Yasutake, Y. Andou, S. Hiki, H. Nishida and T. Endo, *J. Polym. Sci. Polym. Chem.* 2004, **42**, 2621.
45. H. L. Huang, S. H. Goh, D. M. Y. Lai and C .H. A. Huan, *Appl. Surf. Sci.*, 2004, **227**, 373.
46. K. Matyjaszewski, D.A. Shipp, J.L. Wang, T. Grimaud and T.E. Patten, *Macromolecules*, 1998, **31**, 6836.
47. J. H. Xia, X. Zhang and K. Matyjaszewski, *Macromolecules*, 1999, **32**, 4482.
48. X. Zhang, J. H. Xia and K. Matyjaszewski, *Macromolecules*, 2001, **33**, 2340.
49. R. F. Storey, K. A. Shoemake, *Polym. Bull*., 1997, **39**, 393.
50. J.W Mays, *Polym. Commun*, 1990, **31**, 170.
51. J.C. Yang, M.J. Jablonsky and J.W. Mays, *Polymer*, 2002, **43**, 5125.
52. A. Eisenberg, J.S. Kim. *Introduction to Ionomers*, New York, Wiley, 1998.
53. J. Zou, Y. Zhao and W. Shi, *J. Membr. Sci*., 2004, **245**, 35.
54. M. Seiler, *Fluid Phase Equilibria*, 2006, **241**, 155.
55. Y. Pan, Y. Huang, B. Liao, M. Chen, G. Cong and L.M. Leung, *J. Appl. Polym. Sci.* 1997, **65**, 341.
56. B. Vishnupriya, K. Ramya and K. S. Dhathathreyan, *J. Appl. Polym. Sci*., 2002, **83**, 1792.
57. K. Ramya, K. S. Dhathathreyan, *J. Appl. Polym. Sci*., 2003, **88**, 307.
58. J. L. Acota, J. L. Garcia-Fierro, A. Linares and M. J. Casanova, *Polym. Int.*, 2000, **49**, 1534.
59. B. Kosmala, J. Schauer, *J. Appl. Polym. Sci*., 2002, **85**, 1118.
60. K. Matsumoto, T. Higashihara and M. Ueda, *Macromolecules*, 2008, **41**, 7560.
61. K. Xu, K. Li, P. Khanchaitit and Q. Wang, *Chem. Mater.*,2007, **19**, 5937.
62. Z. Shi, Ph.D. Thesis, Simon Fraser University, Burnaby, Canada, 2004.
63. Y.A. Elabd, E. Napadensky, J.M. Sloan, D.M. Crawford and C.W. Walker, *J. Membr. Sci*., 2003, **217**, 227.
64. P.D. Beattie, F.P. Orfino, V.I. Basura, K. Zychowska, J. Ding, C. Chuy, J. Schmeisser and S. Holdcroft, *J. Electroanal. Chem.*, 2001, **503**, 45.
65. P. Batat, C. Bilir, T. Erdogan, A. L. Demirel, *European Polymer Journal*, 2014, **54**, 79